

Development and assessment of a nested enterocyte-cytochrome P450 turnover model and implications for mechanism-based inhibition of gut wall metabolism

A.S. Darwich¹, U. Aslam¹, A. Rostami-Hodjegan^{1,2}

¹Centre for Applied Pharmacokinetic Research, University of Manchester, UK

²Simcyp Ltd, Sheffield, UK

adam.darwich@postgrad.manchester.ac.uk

MANCHESTER
1824

The University of Manchester

simcyp
real solutions from virtual populations

Introduction

Prediction of drug-drug interactions (DDIs), e.g. mechanism-based inhibition (MBI), is an essential application in physiologically-based pharmacokinetic (PBPK) modelling, where small intestinal metabolism plays an important role.

PBPK modelling of MBI in the gut will depend on the level of active enzyme in the gut wall ($A_{\text{Enz-GI}}$), a function of inhibitor concentration ($f_{\text{u,Ent}} \cdot I_{\text{Ent}}$), its maximal rate of enzyme inactivation (k_{inact}), the inhibitor concentration producing half of the maximal rate of inactivation ($K_{\text{I,u}}$). Further, The level of interaction will be determined by the level of active enzyme at steady state ($A_{\text{Enz-GI,SS}}$) and enzyme degradation rate ($k_{\text{deg,Enz}}$; Equation 1) [1-3]:

$$\frac{dA_{\text{CYP-GI}}}{dt} = k_{\text{deg,Enz}} \cdot A_{\text{Enz-GI,SS}} - A_{\text{Enz-GI}}$$
$$\left(k_{\text{deg,Enz}} \cdot \frac{k_{\text{inact}} \cdot f_{\text{u,Ent}} \cdot I_{\text{Ent}}}{K_{\text{I,u}} + f_{\text{u,Ent}} \cdot I_{\text{Ent}}} \right) \quad (\text{Equation 1})$$

Where $k_{\text{deg,Enz}}$ is a surrogate parameter of the combined turnover rate of the enterocyte and enzyme. Enzyme turnover is determines the timeframe and extent of MBI, where some anecdotal evidence have indicated potential overestimations of inhibition of gut metabolism.

Aim and objectives

The aim was to theoretically examine the nesting and hierarchy of enterocyte and CYP3A4 enzyme turnover and its impact on MBIs in the gut wall using a systems pharmacology approach and independent information on enterocyte turnover. This would be carried out through the development and assessment of a nested enzyme-within-enterocyte turnover (NET) model coupled to a minimal PBPK model.

Methods

A nested enzyme turnover (NET) model describing CYP3A4 activity in the gut wall was developed in Matlab R2010a, allowing the simulation of enzyme turnover nested within the enterocyte subject to independent enterocyte turnover (Figure 1 and 2).

Realistic parameter estimates and ranges of $k_{\text{deg,ent}}$, the degradation rate of small intestinal CYP3A4 ($k_{\text{deg,CYP3A}}$), K_{inact} and $K_{\text{I,u}}$, where explored through a simulation based exploratory sensitivity analysis utilising the developed NET model.

Results

The NET model displayed a lower level of inhibition following MBI as compared to the conventional PBPK modelling approach ($k_{\text{deg,Ent}}=0 \text{ h}^{-1}$) as a consequence of an increase in $k_{\text{deg,Ent}}$ and $k_{\text{deg,CYP3A}}$. Inhibitors displaying low $K_{\text{I,u}}$ or high k_{inact} were more likely to give rise to a lower level of inhibition, where a combination of low $K_{\text{I,u}}$ and high k_{inact} led to the lowest level of inhibition using the NET model as compared to the conventional approach (Figure 3 and 4).

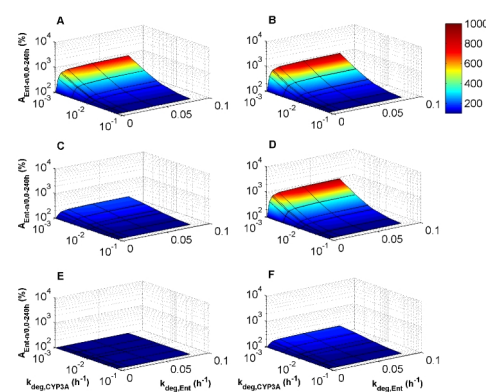


Figure 3. Simulated activity of CYP3A4 in the gastrointestinal tract over 240h following mechanism-based inhibition ($A_{\text{Ent-n}}(0-240\text{h})$ [%] relative to the standard model scenario (enterocyte degradation rate [$k_{\text{deg,Ent}}=0 \text{ h}^{-1}$] in relation to $k_{\text{deg,CYP3A}}$ (h^{-1}) and $k_{\text{deg,Ent}}$ (h^{-1}), varying the maximal rate of enzyme inactivation (k_{inact} (h^{-1}) and the inhibitor concentration producing half of the maximal rate of inactivation ($K_{\text{I,u}}$). A: $K_{\text{I,u}}=0.01 \mu\text{M}$ and $k_{\text{inact}}=1 \text{ h}^{-1}$, B: $K_{\text{I,u}}=0.01 \mu\text{M}$ and $k_{\text{inact}}=150 \text{ h}^{-1}$, C: $K_{\text{I,u}}=5 \mu\text{M}$ and $k_{\text{inact}}=1 \text{ h}^{-1}$, D: $K_{\text{I,u}}=5 \mu\text{M}$ and $k_{\text{inact}}=150 \text{ h}^{-1}$, E: $K_{\text{I,u}}=2000 \mu\text{M}$ and $k_{\text{inact}}=1 \text{ h}^{-1}$, and F: $K_{\text{I,u}}=2000 \mu\text{M}$ and $k_{\text{inact}}=150 \text{ h}^{-1}$.

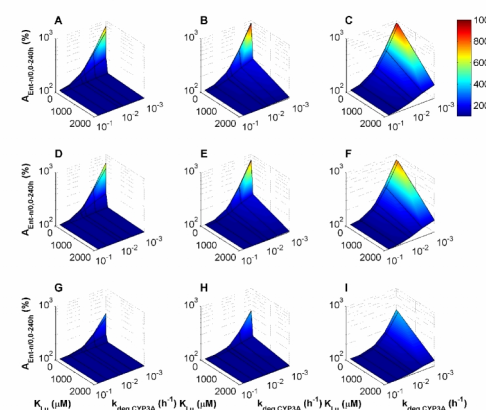


Figure 4. Simulated activity of CYP3A4 in the gut wall over 240h following mechanism-based inhibition ($A_{\text{Ent-n}}(0-240\text{h})$ [%] relative to standard model scenario ($k_{\text{deg,Ent}}=0 \text{ h}^{-1}$) in relation to $K_{\text{I,u}}$ (inhibitor concentration producing half of the maximal rate of inactivation) and $k_{\text{deg,CYP3A}}$ (h^{-1}), varying $k_{\text{deg,Ent}}$ and k_{inact} (maximal rate of enzyme inactivation): A: $k_{\text{deg,Ent}}=0.007 \text{ h}^{-1}$ and $k_{\text{inact}}=10 \text{ h}^{-1}$, B: $k_{\text{deg,Ent}}=0.007 \text{ h}^{-1}$ and $k_{\text{inact}}=150 \text{ h}^{-1}$, C: $k_{\text{deg,Ent}}=0.006 \text{ h}^{-1}$ and $k_{\text{inact}}=10 \text{ h}^{-1}$, D: $k_{\text{deg,Ent}}=0.006 \text{ h}^{-1}$ and $k_{\text{inact}}=150 \text{ h}^{-1}$, E: $k_{\text{deg,Ent}}=0.007 \text{ h}^{-1}$ and $k_{\text{inact}}=10 \text{ h}^{-1}$, F: $k_{\text{deg,Ent}}=0.006 \text{ h}^{-1}$ and $k_{\text{inact}}=150 \text{ h}^{-1}$, G: $k_{\text{deg,Ent}}=0.007 \text{ h}^{-1}$ and $k_{\text{inact}}=10 \text{ h}^{-1}$, H: $k_{\text{deg,Ent}}=0.007 \text{ h}^{-1}$ and $k_{\text{inact}}=150 \text{ h}^{-1}$, and I: $k_{\text{deg,Ent}}=0.006 \text{ h}^{-1}$ and $k_{\text{inact}}=150 \text{ h}^{-1}$.

Results (continued)

In general, the developed NET model was associated with a lower inhibition of small intestinal CYP3A4 activity following MBI as compared to the conventional PBPK modelling approach ($k_{\text{deg,Ent}}=0 \text{ h}^{-1}$).

Comparing the outcome of the NET model on intestinal CYP3A4 activity using observed data of $k_{\text{deg,Ent}}$ (0.01 h^{-1}) and $k_{\text{deg,CYP3A}}$ (0.03 h^{-1}) as compared to the hybrid parameter $k_{\text{deg,CYP3A}}$ (0.04 h^{-1}) in the conventional model, indicated the NET model to display a lower degree of inhibition for a number of MBIs.

The increase in intestinal CYP3A4 activity was further apparent for inhibitors for which overpredictions have been reported utilising a conventional modelling approach, including fluoxetine ($K_{\text{I,u}}=5.19 \mu\text{M}$, $k_{\text{inact}}=1.02 \text{ h}^{-1}$) and mibefradil ($K_{\text{I,u}}=2.23 \mu\text{M}$, $k_{\text{inact}}=24 \text{ h}^{-1}$), displaying approximately 1.13 and 1.31 fold higher activity of intestinal CYP3A4 respectively following MBI (Figure 5).

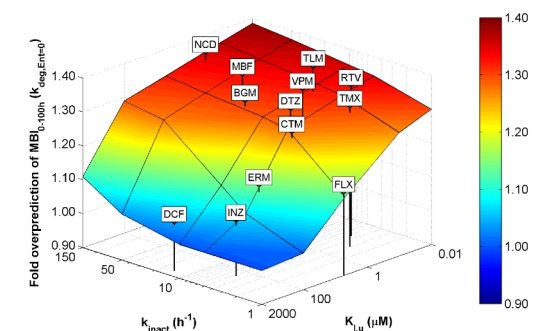


Figure 5. Simulated fold overprediction of mechanism-based inhibition over 100h utilising the NET model, at a CYP3A and enterocyte degradation rate ($k_{\text{deg,CYP3A}}$ and $k_{\text{deg,Ent}}$) of 0.03 h^{-1} and 0.01 h^{-1} respectively, as compared to the conventional PBPK modelling at a $k_{\text{deg,CYP3A}}$ of 0.04 h^{-1} ($k_{\text{deg,Ent}}=0 \text{ h}^{-1}$); in relation to $K_{\text{I,u}}$ (the inhibitor concentration that produces half of the maximal rate of inactivation [μM]) and k_{inact} (the maximal rate of enzyme inactivation). Inhibitors are mapped in accordance to their $K_{\text{I,u}}$ and k_{inact} indicating the relative impact of different model scenarios. FLX=fluoxetine, TMX=tamoxifen, CTM=clarithromycin, RTV=ritonavir, ERM=erythromycin, INZ=isoniazid, VPM=verapamil, DTZ=diltiazem, TLM=troleandomycin, NFV=nelfinavir, DCF=diclofenac, BGM=bergamottin, MBF=mibefradil and NCD=nicardipine.

Discussion and Conclusions

The model displayed potential to improve on predictions of mechanism-based inhibition, producing a lower level of inhibition as compared to the conventional modelling approach.

The utilisation of a more physiological description of small intestinal enzyme and cell dynamics following DDIs has the potential for further application on a number of subpopulations and disease states where the enzyme or enterocyte turnover may be altered.

The developed NET model is, to our knowledge, the first PBPK model to consider the nesting and hierarchy of the enzyme and enterocyte turnover in the small intestine.

Acknowledgements

Authors wish to thank Mr Michael Croucher, University of Manchester, for his assistance with optimising model code.

References

- [1] Fahmi OA, Hurst S, Plowchalk D, Cook J, Guo F, Youdim K, et al. Drug Metab Dispos. 2009;37(8),1658-66.
- [2] Obach RS, Walsky RL, Venkatakrishnan K. Drug Metab Dispos. 2007;35(2),246-55.

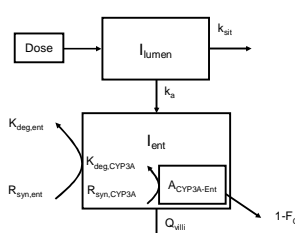


Figure 1. The nested enzyme turnover model describing inhibitor concentrations in: Gut lumen (I_{lumen}) and the enterocytes (I_{ent}). Rates and blood flows include: absorption (k_a) and small intestinal transit rate (k_{si}) and villous blood flow (Q_{vill}). $R_{\text{syn,ent}}$ and $k_{\text{deg,ent}}$ are production and degradation rates of the enterocytes. $R_{\text{syn,CYP3A}}$ and $k_{\text{deg,CYP3A}}$ indicate the turnover of CYP3A4. F_a =fraction of dose that is absorbed through the gut wall, F_G =fraction of absorbed dose that escapes gut wall metabolism

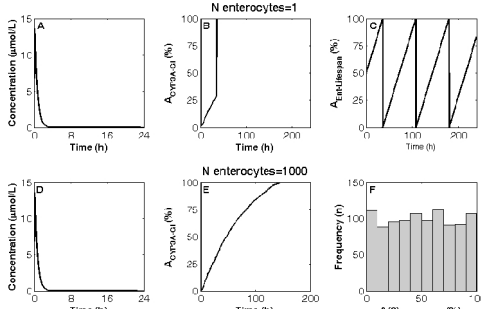


Figure 2. Conceptual simulation of an enterocyte ($n=1$) utilising the nested enzyme turnover model, displaying A: Inhibitor concentration in the enterocyte, B: Relative activity of CYP3A4 in the small intestine ($A_{\text{CYP3A-GI}}$) following mechanism-based inhibition, C: Enterocyte life progression over time. Conceptual simulations of $n=1000$ enterocytes D: Inhibitor concentration in the enterocyte tissue, E: $A_{\text{CYP3A-GI}}$ following mechanism-based inhibition, F: Distribution of initial starting points of the enterocyte population life progression ($A(t=0)_{\text{Ent-Lifespan}}$).